Chemistry Central Journal

ChemistryCentral

Research article

Open Access

Characterisation of different polymorphs of tris(8-hydroxyquinolinato)aluminium(III) using solid-state NMR and DFT calculations

Mithun Goswami, Pabitra K Nayak, N Periasamy† and PK Madhu*†

Address: Department of Chemical Sciences, Tata Institute of Fundamental Research, Homi Bhabha Road, Colaba, Mumbai 400 005, India

Email: Mithun Goswami - mithun@tifr.res.in; Pabitra K Nayak - pabitra@tifr.res.in; N Periasamy - peri@tifr.res.in; PK Madhu* - madhu@tifr.res.in

* Corresponding author †Equal contributors

Published: 9 November 2009

Chemistry Central Journal 2009, **3**:15 doi:10.1186/1752-153X-3-15

Received: 12 May 2009
Accepted: 9 November 2009

This article is available from: http://journal.chemistrycentral.com/content/3/1/15

Abstract

Background: Organic light emitting devices (OLED) are becoming important and characterisation of them, in terms of structure, charge distribution, and intermolecular interactions, is important. Tris(8-hydroxyquinolinato)-aluminium(III), known as Alq_3, an organometallic complex has become a reference material of great importance in OLED. It is important to elucidate the structural details of Alq_3 in its various isomeric and solvated forms. Solid-state nuclear magnetic resonance (NMR) is a useful tool for this which can also complement the information obtained with X-ray diffraction studies.

Results: We report here ^{27}Al one-dimensional (1D) and two-dimensional (2D) multiple-quantum magic-angle spinning (MQMAS) NMR studies of the meridional (α-phase) and the facial (δ-phase) isomeric forms of Alq_3. Quadrupolar parameters are estimated from the 1D spectra under MAS and anisotropic slices of the 2D spectra and also calculated using DFT (density functional theory) quantum-chemical calculations. We have also studied solvated phase of Alq_3 containing ethanol in its lattice. We show that both the XRD patterns and the quadrupolar parameters of the solvated phase are different from both the α-phase and the δ-phase, although the fluorescence emission shows no substantial difference between the α-phase and the solvated phase. Moreover, we have shown that after the removal of ethanol from the matrix the solvated Alq_3 has similar XRD patterns and quadrupolar parameters to that of the α-phase.

Conclusion: The 2D MQMAS experiments have shown that all the different modifications of Alq_3 have ^{27}Al in single unique crystallographic site. The quadrupolar parameters predicted using the DFT calculation under the isodensity polarisable continuum model resemble closely the experimentally obtained values. The solvated phase of Alq_3 containing ethanol has structural difference from the α-phase of Alq_3 (containing meridional isomer) from the solid-state NMR studies. Solid-state NMR can hence be used as an effective complementary tool to XRD for characterisation and structural elucidation.

Background

In organic based semiconductor devices, molecular solids of organic molecules are used in active layers [1]. The properties of amorphous solid thin films can be different from the properties of isolated molecule, due to interaction among the molecules in solid state. The properties of amorphous solid thin films are mainly decided at the molecular level and modulated by intermolecular interactions and other bulk properties. Hence, it is important to have information about the structure of the organic molecule, charge distribution on the molecular framework, and intermolecular interactions as they collectively govern the performance of the device.

Following the experimental demonstration by Tang *et al*. [2] Tris(8-hydroxyquinolinato)- aluminium(III), known as Alq_3, has become a workhorse material for organic light emitting devices (OLED) and/or electron transporting material in OLED. Alq_3 is an octahedrally coordinated chelate complex, with an Al^{3+} ion in the center and three 8-hydroxyquinolinate ions octahedrally coordinated around it. It has mainly two types of geometrical isomeric forms, meridional and facial. Brinkmann *et al*. investigated the light emitting properties of the isomeric states and the polymorphs of Alq_3 and determined that molecular packing plays a significant role [3]. X-ray diffraction studies showed that the two crystalline polymorphs of Alq_3, α and β forms, are mainly composed of the meridional isomer [3]. Recently a new crystalline phase of Alq_3, namely δ-Alq_3, was discovered [4]. It shows blue luminescence which is markedly different from the meridional isomer which shows green luminescence. The quantum yield is also higher in the δ-phase. These results suggest that there is a clear correspondence between the crystal structure of Alq_3 and the photoluminescence property. Extensive studies on the δ-phase of Alq_3 have been carried out and it was suggested that δ-Alq_3 is composed purely of facial Alq_3 [5,6]. Again in the case of charge carrier transport in Alq_3, intermolecular interactions play the most crucial role [7]. Also, it has been a practice to use different dopants in Alq_3 emitting layers to obtain desired colours [1]. Such Alq_3 systems which accommodate small solvent molecules within its crystal matrix are in general known as solvated Alq_3. It was also reported that the unit crystal structure and the crystal packing change in Alq_3 when it hosts small solvent molecules, which resulted in a small red shift in the fluorescence spectra [3].

Considering the above stated facts, it becomes important to have insight about the structure of Alq_3 in both the solvated and the unsolvated form and about the in-tramolecular and intermolecular interactions. Though X-ray diffraction is a powerful tool to yield insight into the structure of crystalline material, solid-state NMR can be as good in providing similar information. In addition, solid-state NMR is particularly suitable for studying disordered or amorphous materials [8-13]. Since Alq_3 has an Al^{3+} ion in the centre, one can make use of it as a probe to monitor the electronic distribution in the molecule. ^{27}Al is well suited for solid-state NMR because of its high natural abundance (100%) and relatively large gyromagnetic ratio. Since ^{27}Al has spin $I = 5/2$, it possesses a quadrupolar moment [14]. It is possible to record and analyse solid-state ^{27}Al MAS NMR spectra, observing the central $m = +1/2 \leftrightarrow -1/2$ magnetic transition under magic-angle spinning (MAS), which, for well-resolved spectra, exhibits a characteristic second-order order broadening. High-resolution quadrupolar spectra can be obtained with two-dimensional (2D) methods such as multiple-quantum MAS (MQMAS) [15]. This can help in identifying the various quadrupolar sites in a system and in obtaining the quadrupolar parameters [16,17]. The study of quadrupolar parameters with solid-state NMR can provide a wealth of information about the local environment around quadrupolar nuclei, as the quadrupolar parameters show strong dependence on the neighbouring electronic environment [14,18].

Octahedral chelate complexes, which are structurally similar to Alq_3, were studied by Schurko and co-workers using one-dimensional (1D) ^{27}Al MAS NMR spectroscopy [19]. They showed that the change of structural environment about the aluminium centres can be easily investigated by studying the quadrupolar parameters of ^{27}Al nuclei of the organic chelate complexes. They also reported how the distortion in the chelate rings leads to larger value of quadrupolar coupling constant in one of the complexes.

Recently Utz *et al*. [10,11] have successfully used 1D MAS ^{27}Al spectroscopy to differentiate between the α phase and the δ phase of Alq_3 and to characterize the structural disorder of amorphous Alq_3 deposited from vapour phase at different rates. They also estimated the EFG tensor on the basis of point charge model and predicted the asymmetry parameters of the α and the δ phase [10]. Kaji *et al*. have done a similar study by recording 1D ^{27}Al spectra under static and MAS condition to characterise the α phase, the δ phase, and the γ phase of Alq_3 and also amorphous Alq_3 [20]. However unlike Utz *et al*. they have used DFT based quantum-chemical calculations to theoretically predict the value of the asymmetry parameters of the α phase and the γ phase. Their study suggested that whilst the α phase contains a non axially symmetric isomer both the δ phase and the γ phase of Alq_3 contain an axially symmetric form.

Here, we have investigated three types of Alq_3 samples: (a) α phase (containing the meridional isomer), (b) δ phase (containing the facial isomer), and (c) solvated phase (containing ethanol in the crystal lattice) using solid-state

NMR combined with density functional theory (DFT) [21] based quantum chemical calculation. We show with MQMAS experiments that in all the polymorphs, ^{27}Al is present in a single crystallographic site. We further demonstrate that the local environment around ^{27}Al in solvated phase is different from that in the α phase with the use of both 1D MAS and 2D MQMAS experiments. We also made use of DMFIT [22] program to model the 1D MAS spectra of all the polymorphs to extract the quadrupolar parameters and we have compared the results with the previous works. In addition the anisotropic slices of the peaks in 2D MQMAS spectra were modelled using the DMFIT program to extract the quadrupolar parameters and isotropic chemical shifts. We further report the result obtained from DFT based quantum-chemical calculation done on isolated molecule and show that the correspondence with the experimental results improve when the calculation is done under the solvation model.

Experimental

Preparation of Alq_3 and X-ray diffraction measurements

Alq_3 was prepared from 8-hydroxyquinoline and $Al(NO_3).9H_2O$ using an aqueous route by a standard procedure [23]. Briefly the procedure adopted was as follows: 1 g of aluminium nitrate $(Al(NO_3)_3).9H_2O$ was dissolved in 100 ml of water. The solution was warmed to 60°C. 1.5 g of 8-hydroxyquinoline was dissolved in a solvent mixture of 20 ml of water and 4 ml of glacial acetic acid. 8-hydroxyquinoline solution was slowly added to aluminium nitrate solution. The pH of the resulting solution was then increased to 8 by the addition of ammonia to precipitate Alq_3 out. The resulting precipitate was washed by hot (60°C) water. The bright yellow powder was dried in oven for overnight. Yield of Alq_3 obtained by this method was 95-100% with a melting point > 300°C. This procedure was adapted from Vogel [24].

Alq_3, as prepared, was subjected to train sublimation under vacuum and purified [23]. Alq_3 gets deposited in different temperature zones. The portion which was deposited at ~175°C was collected. Powder XRD pattern of the sample matched with the reported pattern for the α phase of Alq_3 [3], which is well established to be the meridional isomer of Alq_3. Fluorescence emission spectra in thin film showed a maximum at 510 nm (Figure 1). Facial isomer of Alq_3 was prepared by thermal annealing process [25]. A quartz tube with N_2 gas flow arrangement at high pressure was used in the preparation. The temperature of the tube was regulated by a heater coil. Alq_3, purified by train sublimation (containing α and other phases of Alq_3), was loaded on an alumina boat kept inside the chamber. The chamber was flushed with N_2 for 2 hrs. The pressure was kept at 1.5 atm. The temperature of the chamber was increased from room temperature to 350°C at the rate of 10°C/min. The temperature was then further

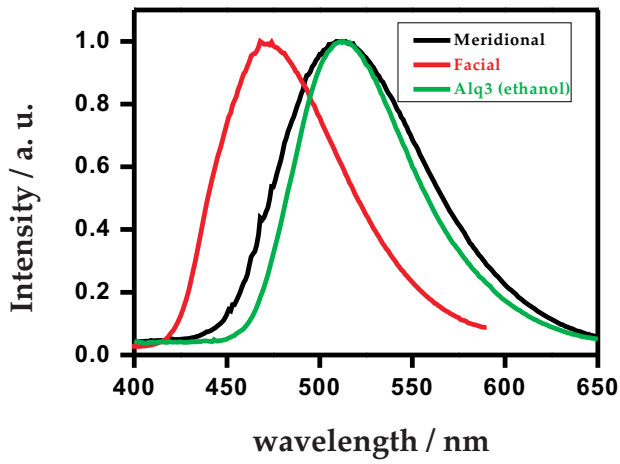

Figure 1
FThe fluorescence emission spectra of a thin film of the α-phase of Alq_3 (meridional), the δ-phase of Alq_3 (facial), and the solvated Alq_3 containing ethanol.

increased to 400°C at the rate of 1°C/min. The system was kept at this temperature for 30 minutes. Temperature of the sample was then brought down to room temperature rapidly by removing it from the heating zone under continuous flow of N_2. A suspension of the annealed sample was made with acetone (7 mg/ml). The suspension was kept for 24 hours with occasional shaking. The suspension was centrifuged at 13000 r.p.m. The grayish-white sample obtained at the bottom of the centrifuge tube was dried over vacuum and kept in glass vials for further study. Powder XRD pattern of the δ phase of Alq_3 matched with the previously reported pattern [5]. Fluorescence emission spectra in thin film showed a maximum at 468 nm (Figure 1). XRD pattern and fluorescence spectrum confirmed the sample to be the facial isomer of Alq_3. The ethanol solvated phase was prepared by recrystallising Alq_3 from ethanol. Fluorescence emission spectra in thin film showed a maximum at 510 nm (Figure 1). Powder XRD pattern showed a close resemblance with the reported solvated phase of the form Alq_3 $(C_6H_5Cl)_{1/2}$ where C_6H_5Cl acts as an inclusion or guest compound within Alq_3 crystal [3]. Alq_3-ethanol solvated phase was annealed at ~200°C under nitrogen atmosphere for 2 hrs to remove ethanol from the crystal lattice. X-ray powder diffraction data were obtained with Philips instrument (panalytica) with a Cu Kα (λ = 1.5418A°) radiation source. Data were recorded at room temperature in 2θ mode ($\Delta 2\theta = 0.017$).

Fluorescence measurements

Steady-state fluorescence of powdered Alq_3 samples was recorded at room temperature using a Spex Fluorolog

fluorimeter. The excitation wavelength was 340 nm and scanned at a step of 1 nm.

Thermo-gravimetric measurements

Thermo-gravimetric analysis (TGA) and differential thermal analysis (DTA) were performed with a NETZSCH instrument. The temperature was varied at 5 K/min under nitrogen atmosphere.

NMR experiments

All NMR experiments were carried out on a Bruker Avance 500 MHz spectrometer operating at a field strength of 11.7 T with a Bruker 4 mm triple-resonance probe. Experiments were performed observing the central transition of ^{27}Al (I = 5/2) resonance of the different forms of Alq_3 sample at a Larmor frequency of 130.28 MHz. Magic-angle spinning was performed at 10 kHz. The nutation frequency of the excitation pulse for the 1D MAS experiments was 120 kHz. For the 2D experiments the split-t_1 sequence proposed by Brown and Wimperis was used [26]. A nutation frequency of 80 kHz was applied for excitation and conversion pulses. The echo time was 2.5 ms. The pulse width of the selective 180° pulse was 27.8 μs. Further experimental details are given in the figure captions of Figs. Three-Six. The chemical shifts were referenced to aqueous 1 M $AlCl_3$ solution. The isotropic quadrupolar shifts from the MQMAS spectra, ν_Q^{iso}, were calculated using the method given in Ref. [16]. In all the experiments swept-frequency two pulse phase modulation (SW_f-TPPM) [27] heteronuclear dipolar scheme was applied to remove the ^{1}H-^{27}Al dipolar couplings [28].

Computation

Density functional theory (DFT) was used in all the quantum-chemical calculations using Gaussian 03 [29]. The DFT method used here is based on hybrid B3LYP functional. The geometry optimisation of Alq_3 (both the facial and the meridional isomer) was done using 6-31G(d) basis set for all the atoms. The gas phase geometry optimised structure was used to calculate the electric field gradients (EFG). The EFG calculation was done using DFT with B3LYP functional. 6-31G(d) basis functions for C, H atoms and 6-311+G(3df) basis set for Al, N and O atoms were taken during the calculation. The more diffused basis sets were used for Al, N, and O due to our interest in the quadrupolar parameters at the Al center of Alq_3. The calculated values are given in Table 1. In organic powder/thin-film samples the organic molecule can be considered as solvated by the molecules of its own type. Hence, it is more realistic to take solid "solvation" into account whilst doing the EFG calculation for the molecules in thin films. For this, the isodensity polarisable continuum model (IPCM) provides an efficient way to consider the solvent effect as it defines the molecular cavity as a contour surface of constant electron probability density of the molecule [30]. Our theoretical calculation of dielectric constants, ε, for facial and meridional isomers came out to be 2.62 and 2.69 respectively. Dielectric constant of a material can be obtained from Clausius-Mossoti equation [31]:

$$\frac{\varepsilon-1}{\varepsilon+2} = 4\pi\rho N_A\alpha / 3M$$

where α is the isotropic polarisability, ρ is the density, M is the molecular mass, N_A is the Avogadro number, and ε is the dielectric constant. Isotropic polarisability (α) and reciprocal of Molar volume (ρ/M) were calculated from geometry optimised structure of the isomers using the DFT method (B3LYP/6-31G (d)). The experimentally determined value of ε for thin film, which predominantly contains the meridional isomer, was found to be 3.0 ± 0.3 [32]. As the computationally determined values for both the isomers were nearly the same, the experimentally determined value of ε for thin film was used in the IPCM calculation for both the isomers. The levels of basis functions were the same for both the gas phase and the solid solvated phase.

Table 1: The ^{27}Al quadrupolar parameters obtained from the DFT quantum-chemical calculation under the isolated molecule and the isodensity polarisable continuum model (IPCM).

Model	Isomer	δ_{iso}(ppm)	η_Q	χ/MHz
Isolated Molecule	α-Alq_3	-	0.77	7.7
	δ-Alq_3	-	0.03	7.0
IPCM	α-Alq_3	-	0.81	7.2
	δ-Alq_3	-	0.10	5.8

Results and discussion

We present here the results obtained from the α and the δ forms of Alq_3 and also from the solvated phase of Alq_3 using 1D MAS and 2D MQMAS NMR experiments. The quadrupolar parameters were obtained by fitting the 1D MAS spectra and the anisotropic slices of the 2D spectra of the three phases using the DMFIT program. We also report the theoretically calculated values of the quadrupolar parameters using the DFT calculations of the α and the δ forms of Alq_3.

NMR and XRD of isomeric forms of Alq_3

Figure 2a shows the comparison between the experimental 1D spectra of the α-phase and 2b shows the δ-phase of Alq_3 with the theoretical line generated using the DMFIT program which gave the quadrupolar coupling constant

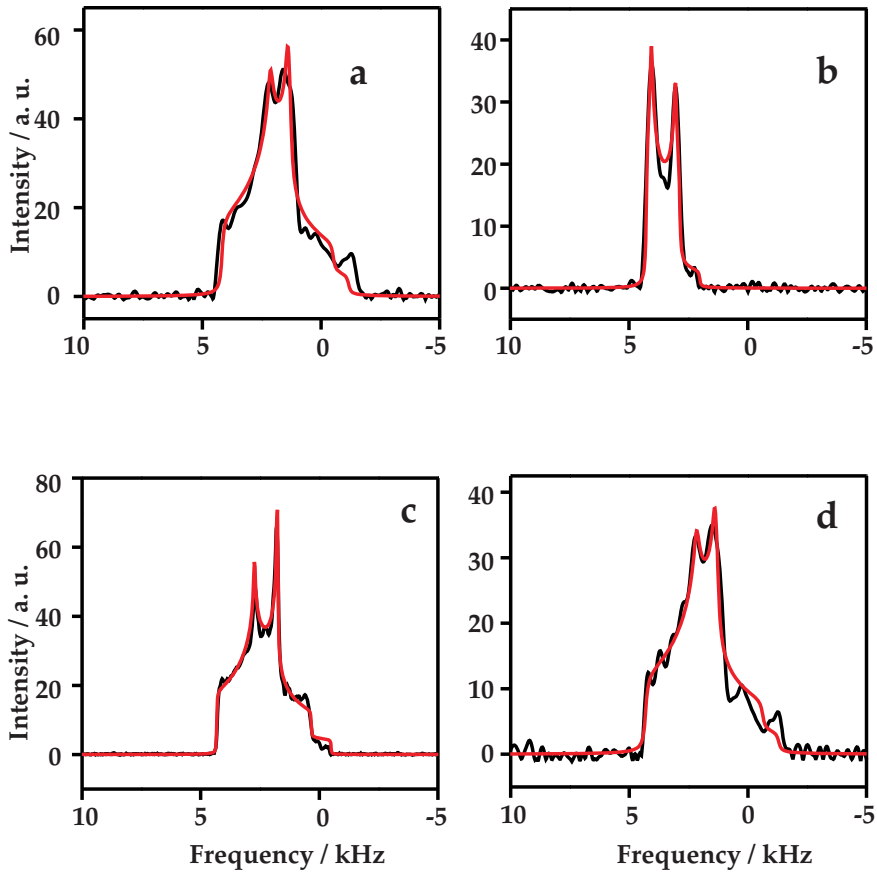

Figure 2
1D ^{27}Al spectra of different modifications of Alq_3 under MAS. Experimental data (black) and fitted spectra (red) of (a) α-Alq_3, (b) δ-Alq_3, (c) solvated Alq_3, and (d) solvated Alq_3 after the removal of ethyl alcohol.

(χ) in MHz, the asymmetry parameter (η_Q), and the average value of isotropic shift which is a combination of both the isotropic chemical shift (δ_{iso}) and the isotropic quadrupolar shift. The uncertainties in the values of χ, η_Q, and δ_{iso} were estimated by visual comparison of experimental and modelled spectra by employing small changes in the parameters and observing the matching of modelled spectra with the experimental ones.

The quadrupolar parameters obtained from the 1D spectra (Table 2) conclusively prove that Al^{+3} ion is situated in an axially symmetric environment in the δ-phase whilst it is in a non-axially symmetric environment in the α-phase of Alq_3. (A low asymmetry value generally signifies axial symmetry and a high asymmetry value denotes otherwise.) This agrees well with the previously reported results [10,11,20]. Figs. 2c and 2d show the 1D spectrum of sol-

Table 2: The ^{27}Al quadrupolar parameters obtained from the 1D MAS and the 2D MQMAS experiments using the DMFIT program.

Experiment	Isomer	δ_{iso}(ppm)	η_Q	χ/MHz
1D MAS	α-Alq_3	55.4 ± 1.0	0.80 ± 0.04	7.0 ± 0.1
	δ-Alq_3	43.6 ± 1.0	0.18 ± 0.03	4.9 ± 0.1
	Solvated Alq_3	50.5 ± 1.0	0.62 ± 0.04	6.4 ± 0.1
	Solvated Alq_3 after the removal of ethanol	55.1 ± 2.0	0.85 ± 0.05	6.5 ± 0.3
2D MQMAS	α-Alq_3	54.7 ± 1.0	0.85 ± 0.04	6.9 ± 0.1
	δ-Alq_3	43.1 ± 1.0	0.15 ± 0.03	5.1 ± 0.1
	Solvated Alq_3	50.4 ± 1.0	0.60 ± 0.04	6.4 ± 0.1
	Solvated Alq_3 after the removal of ethanol	55.0 ± 2.0	0.81 ± 0.04	6.9 ± 0.3

vated Alq_3 before and after removal of the ethanol respectively along with the fitted lines. The 1D spectra of the α-phase of Alq_3, the δ-phase of Alq_3, and the solvated Alq_3 have distinctly different second-order quadrupolar broadened line shapes. The quadrupolar parameters obtained using the DMFIT program also show significant difference between the α-phase and the solvated Alq_3, which clearly suggests that the introduction of an ethanol molecule inside the Alq_3 matrix changes the local environment around Al^{+3} in the centre. Further, the line shape of the apohost Alq_3 (i.e, after the removal of ethanol from the solvated phase) has similar features to that of the α-phase of Alq_3 which is also evident from their nearly similar quadrupolar parameters (Table 2).

Figs. 3, 4, 5, and 6 show the 2D 3QMAS spectrum of the α phase, the δ phase, and the solvated phase before and after the removal of ethanol respectively of Alq_3. Sidebands appear along the F_1 dimension of the 2D spectra as the t_1 increments were not synchronised with the MAS rotor period. The isotropic spectrum is obtained from a projection on to F_1 which in all cases consists of only a single resonance. This indicates that all the phases studied here have ^{27}Al in an unique crystallographic site. The cross section extracted along the ridge line shape parallel to the F_2 axis was fitted using the DMFIT program. From the fit the quadrupolar parameters were extracted and are given in Table 1. Figure 7 shows a comparison of the 2D MQMAS experimental anisotropic slice with the theoretical line generated using the DMFIT program. Since the DMFIT program gives the model spectrum of a site under ideal excitation, there will be some difference in the line shapes of the model and the experimental spectra, nevertheless the procedure for the model calculation is quite robust and gives fairly accurate results [22].

The quadrupolar parameters in Table 2 indicate that the α phase of Alq_3 contains only the meridional isomer as reported from the XRD study [3] and the δ phase of Alq_3 is composed of purely facial isomer as reported from the XRD study [5].

From Figs. 5 and 6, it can be observed that the isotropic projection for solvated Alq_3 is much narrower compared to the α-phase, the δ phase, and the solvated Alq_3 from which ethanol was removed. It is well known that chemical and/or rotational exchange processes can influence the powder patterns of half-integer spin quadrupolar nuclei [33]. In general, the higher the rate and symmetry of the exchange process the narrower will be the line width. Hence, the reason for the narrowing down of isotropic projection of solvated Alq_3 could be due to the high mobility of the quinoline ligands between chemically equivalent orientations around the ^{27}Al site due to the introduction of ethanol into the crystal structure. Also it was observed that the shape of the cross section extracted along the F_2 dimension of the solvated Alq_3 is completely different from that of the α-phase of Alq_3 which was earlier indicated by their 1D MAS spectra as well. This also clearly indicates that the local electronic environment

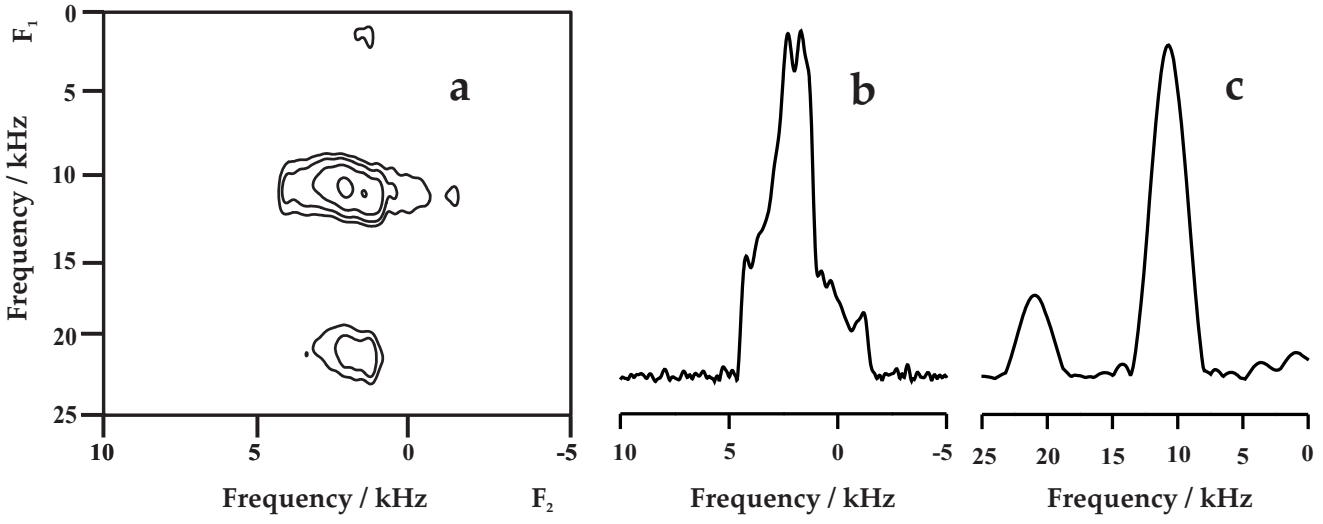

Figure 3
(a) 2D 3QMAS spectra of meridional Alq_3 (α-phase). The optimized excitation pulse and conversion pulse lengths were 3.8 μs and 1.8 μs. A total of 64 t_1 increments was taken with 10 μs of dwell time with 288 transients per increment. The recycling delay was 1 s. Total experiment time was 5 hours. (b) The anisotropic slice along the direction parallel to the F_2 dimension. (c) The isotropic projection along the F_1 dimension.

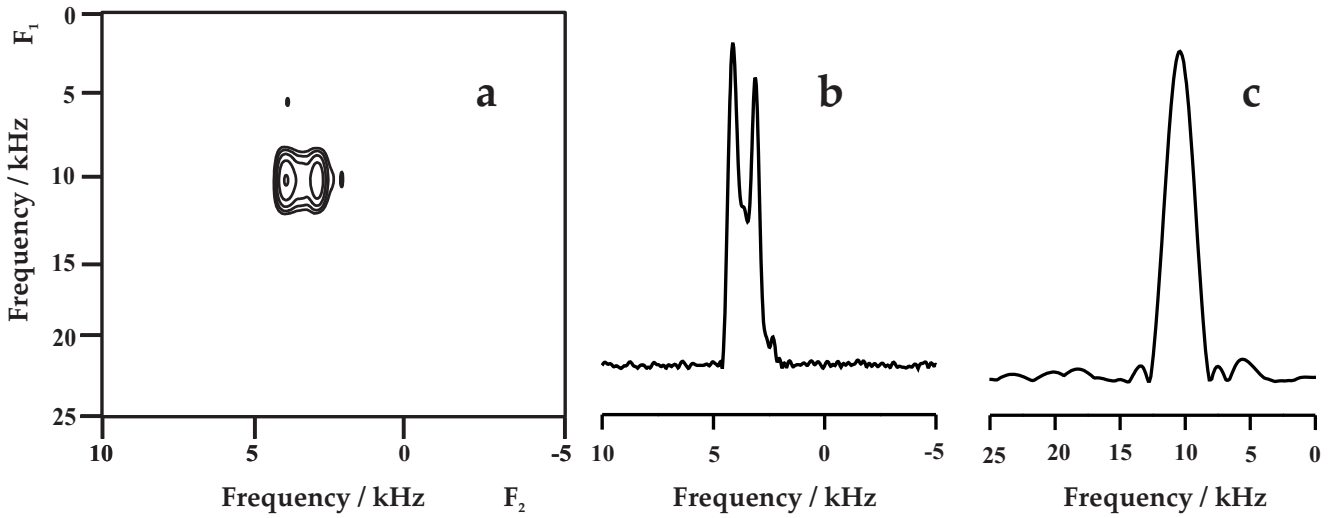

Figure 4
(a) 2D 3QMAS spectra of facial Alq_3 (δ-phase). The optimised excitation pulse and conversion pulse lengths were 4.4 μs and 1.9 μs. Rest of the experimental parameters are as in Figure 3. (b) The anisotropic slice along the direction parallel to the F_2 dimension. (c) The isotropic projection along the F_1 dimension.

around the ^{27}Al centre undergoes significant change upon the introduction of ethanol into the matrix. Similar results were reported by Brinkmann *et al*. [3] where they showed that the unit crystal structure of the α-phase (triclinic) is different from that of a solvated phase of the form $Alq_3(C_6H_5Cl)_{1/2}$ (monoclinic). On the other hand the fluorescence emission spectra (Fig. 1) interestingly show practically no difference between the α-form (meridional) of Alq_3 and the solvated Alq_3 containing ethyl alcohol. It shows fluorescence in Alq_3 is determined at molecular level and hardly influenced by molecular packing. Further the shape of the anisotropic slice of the apohost Alq_3 has remarkable resemblance to that of the α-phase. However, the isotropic projection is broader in the apohost form compared to the later. In a recent study on the polymorphism of a hexa-substituted benzene derivative, Hexakis

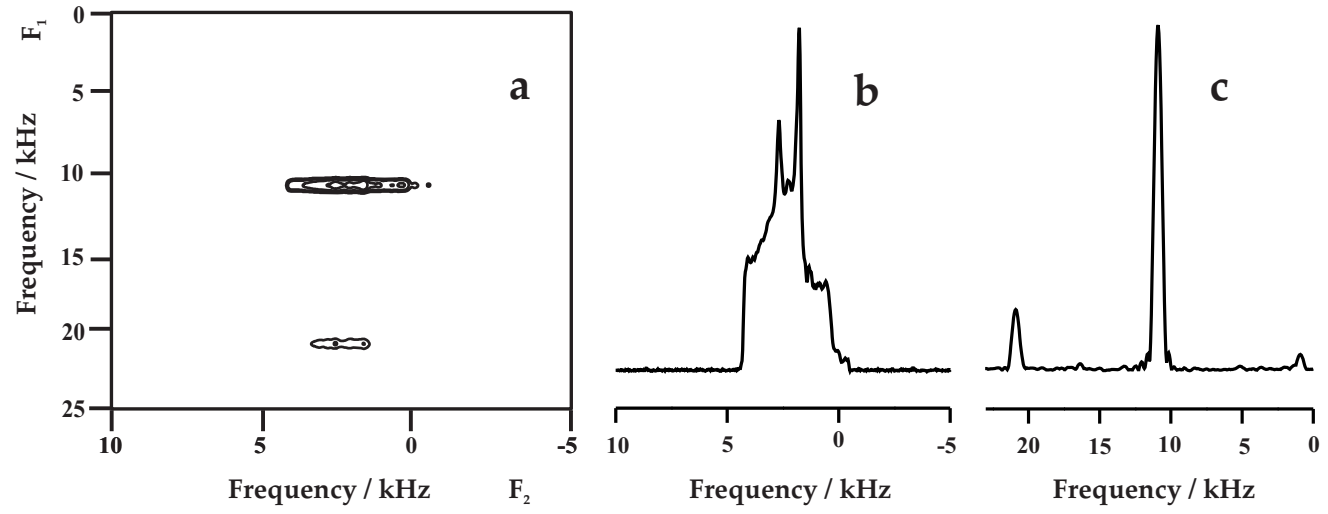

Figure 5
(a) 2D 3QMAS spectra of solvated Alq_3 (containing ethanol). Optimised excitation and conversion pulse lengths were 4.6 μs and 2.5 μs. A total of 192 t_1 increments was taken with 8 μs of dwell time with 96 transients per increment. The recycling dealy was 1 s. Total experiment time was 5 hours 18 mins. (b) The anisotropic slice along the direction parallel to the F_2 dimension. (c) The isotropic projection along the F_1 dimension.

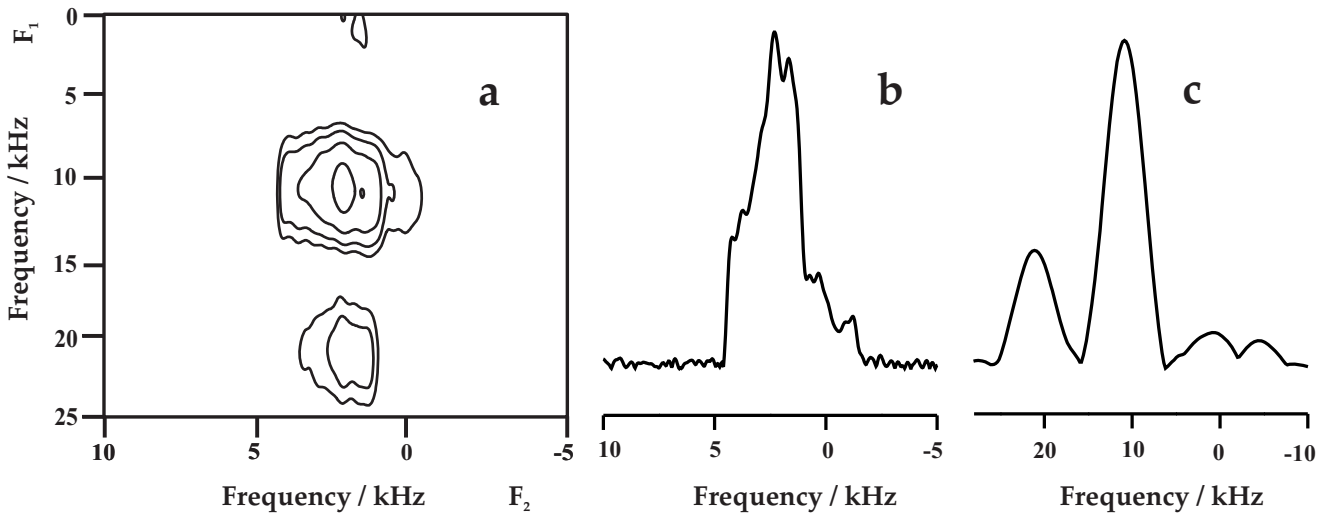

Figure 6
(a) 2D 3QMAS spectra of solvated Alq_3 after the removal of ethanol. Optimised excitation and conversion pulse lengths were 3.8 μs and 1.8 μs. A total of 60 t_1 increments was taken with 5 μs of dwell time with 576 transients per increment. The recycling dealy was 1s. Total experiment time was 9 hours 42 mins. (b) The anisotropic slice along the direction parallel to the F_2 dimension. (c) The isotropic projection along the F_1 dimension.

(4-cyanophenyloxy) benzene, it was suggested that one can get four different polymorphic forms of the above mentioned compound when crystallising it from melt [34]. It can be argued qualitatively that removal of ethanol from the solvated Alq_3 is akin to the process of crystallising from melt, as the number of ethanol molecules existing per unit Alq_3 to solvate it is very small. Therefore it is possible that more than one polymorph may appear from the re-crystallisation process giving rise to a distribution of NMR parameters resulting in the broadening of the ridges in the 3QMAS experiments. The quadrupolar parameters obtained for the α-phase of Alq_3 and the apohost Alq_3 are similar to each other indicating a similar environment around ^{27}Al in the two forms. Similar observations were also made from the XRD analysis, Figure 8, where the solvated form of Alq_3 containing ethanol has distinctly different feature from that of the α-phase. However, when the ethanol was removed from the solvated phase it gave XRD feature similar to that of the α-phase.

Figure 9 shows the data from the thermo gravimetric analysis of the solvated phase indicating a mass loss of 9.4% at 185°C which corresponds to loss of one molecule of ethanol from $Alq_3(C_2H_5OH)_1$. It should be noted that Mq_3 where M is a trivalent metal can host small molecules in its solvated phase [3]. The removal of ethanol at a temperature higher than its boiling point confirms its participation in the crystal lattice. Though ethanol is not chemically bonded to Alq_3 its presence within the lattice affects the electronic distribution around Al and as a result the quadrupolar parameters of the solvated phase are different from either the α or the δ phase.

Quantum-chemical calculation

Quantum-chemical calculations yield principal components of EFG tensor, q_{ii}, in atomic unit, with $|q_{zz}| \geq |q_{yy}| \geq |q_{xx}|$. The calculated q_{ii} values were used to obtain the quadrupolar parameters manually [17],

$$\chi = e^2 Q q_{zz} / h$$

$$\text{Asymmetry parameter } \eta_Q = |(q_{yy} - q_{xx}) / q_{zz}|, 0 \leq \eta_Q \leq 1$$

where Q is the quadrupolar moment of ^{27}Al nuclei. The atomic Q(^{27}Al) value is $14.66 \times 10^{-30} m^2$ [35]. The calculated values of quadrupolar parameters are tabulated in Table 1.

DFT calculation of EFG principal values were done for isolated Alq_3 molecule. The asymmetry parameter η_Q obtained for the α-form was 0.77 while η_Q for the δ-phase of Alq_3 came to be 0.03. Previously Kaji *et al*. [20] also did similar kind of DFT calculations where they predicted that the η_Q values for the α-form and the γ form of Alq_3 are 0.72 and 0.0 respectively. They also reported that the DFT calculation for the δ-phase yielded inconsistent results. Utz *et al*. [11] carried out a simple calculation for the estimation of EFG tensor on the basis of the assumption that the EFG tensor is determined by three point charges of *-e* at the oxygen sites. However, the values of η_Q predicted by this model (0.91 for meridional and 0.26 for facial) over-

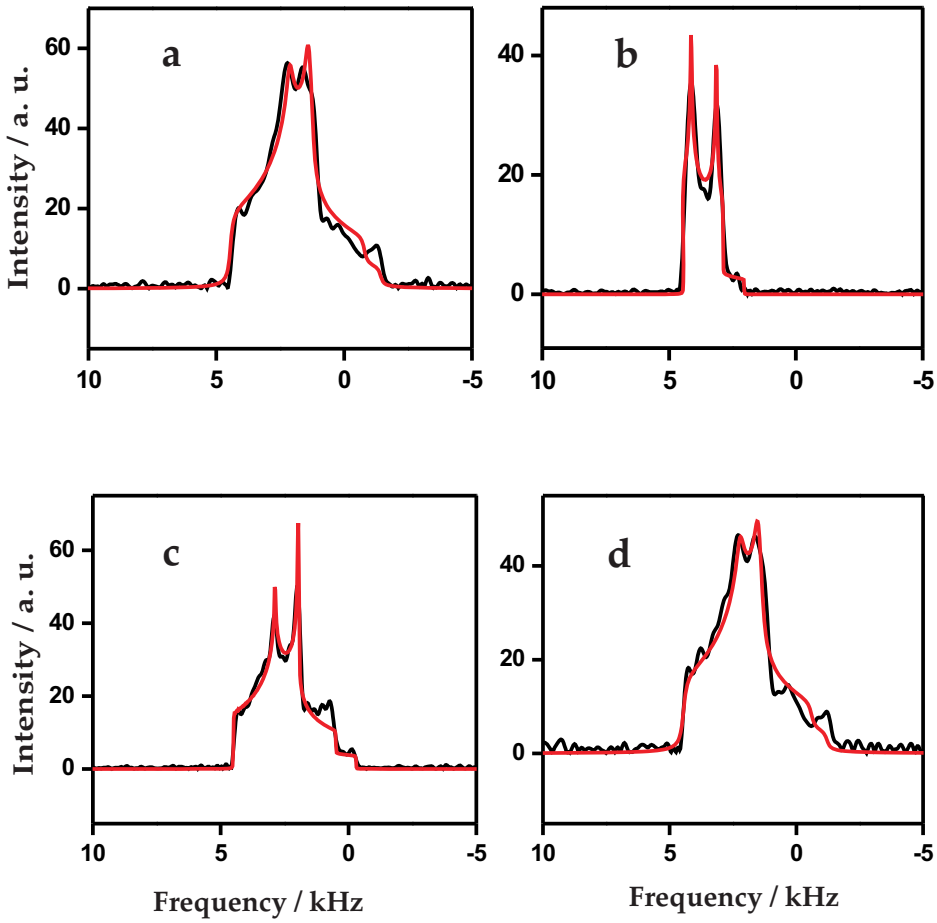

Figure 7
Comparison between 2D MQMAS (black) and fitted (red) line shapes for (a) meridional (α-phase), (b) facial (δ-phase), (c) solvated Alq_3 containing ethanol, and (d) after the removal of ethanol from the solvated Alq_3.

shoot the experimental values obtained by us for both the isomers.

Here we propose a model for DFT calculation where molecules are considered under the influence of a continuum dielectric medium (IPC model) which is a more realistic situation. Under this model it is observed that the theoretically predicted values (0.81 for meridional and 0.10 for facial) show a relatively good agreement with the experimental values. In the case of solvated Alq_3, it was not possible to take a suitable model for the DFT calculation.

Conclusion

We have performed 1D MAS and 2D MQMAS experiments to obtain high-resolution spectra of meridional (α-phase) and facial (δ-phase) isomers of Alq_3. We have determined the quadrupolar parameters from 1D MAS spectra using the DMFIT program. The 2D MQMAS experiments have shown that all the different modifications of Alq_3 have ^{27}Al in single unique crystallographic site which is evident from the single isotropic peak along F_1 dimension. The quadrupolar parameters were also predicted using the DFT calculation under isolated molecule assumption and also under the IPC model. The theoretically calculated values of quadrupolar parameters improve and come close to the experimentally obtained values when calculations are done under the IPC model where an Alq_3 molecule is assumed to be solvated in a surrounding of similar Alq_3 molecules, which is the closest to the actual situation. Solid-state NMR data indicate that the solvated phase of Alq_3 containing ethanol has structural difference from the α-phase of Alq_3 (containing meridional isomer). This was also confirmed by the XRD features, though the fluorescence spectra did not show any significant difference between them which again reaffirms the fact that fluorescence is determined at molecular level in Alq_3 and does not depend on the crystal structure. Further the isotropic projection of the solvated Alq_3 is much narrower than all the other polymorphs, which could be due to dynamic exchange processes. Thermo-

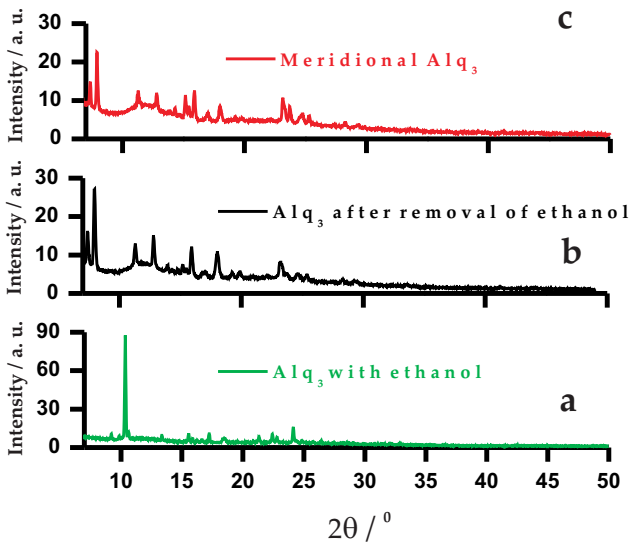

Figure 8
XRD data of (a) solvated Alq_3, (b) after the removal of ethanol, and (c) the α-phase of Alq_3 (meridional).

gravimetric analysis show that there is one ethanol molecule per Alq_3 in the solvated form. After the removal of ethanol the solvated Alq_3 becomes structurally similar to the α-phase of Alq_3. However, due to the possible introduction of more than one polymorph during re-crystallisation, broader ridges appear in the 2D 3QMAS spectrum of the apohost Alq_3. Solid-state NMR can hence be used as an effective complementary tool to XRD for characterisation and structural elucidation. A more realistic approach to the calculation of the EFG tensor would be to consider

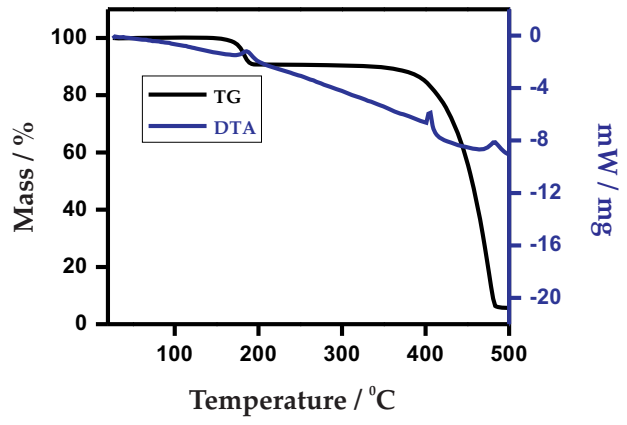

Figure 9
Thermo-gravimetric analysis (TGA) and differential thermal analysis (DTA) plots of solvated Alq_3 containing ethanol.

the molecule to be solvated by similar molecules (IPC model).

During the review process of this manuscript similar findings were published by Nishiyama *et al*. [36]. They report two distinct sites for α-Alq_3 which is at variance to our observation. This could be due to the differences in the sample preparation conditions as it seems Nishiyama *et al*. have collected all the portions from the train sublimations whilst we have collected the portions from a hot region (~170°C) and near the sublimation boat. The α-Alq_3 sample in the current work was also characterised by powder XRD.

Competing interests
The authors declare that they have no competing interests.

Authors' contributions
PKN prepared the samples and carried out all the non-NMR experiments, MG performed the NMR experiments and data analysis, PKN and MG conceived of the DFT studies and implemented them, NP and PKM conceived the study, PKM drafted the manuscript, and all authors read and approved the final manuscript. PKN and MG contributed equally to this manuscript.

Acknowledgements
We acknowledge the use of National Facility for High-Field NMR, TIFR, for the use of the Bruker AV500 spectrometer, Thomas Bräuniger for discussions and a careful reading of the manuscript, and M. V. Naik for technical assistance.

References
1. Adachi C, Tsutsui T: *Organic Light Emitting Devices* Edited by: Shinar J. NewYork: Springer-Verlag; 2004.
2. Tang CW, Van Slyke SA: **Organic electroluminescent diodes.** *Appl Phys Lett* 1987, **51:**913-916.
3. Brinkmann M, Gadret G, Muccini M, Taliani C, Masciocchi N, Sironi A: **Correlation between molecular packing and optical properties in different crystalline polymorphs and amorphous thin films of mer-tris(8-hydroxyquinoline)aluminum(III).** *J Am Chem Soc* 2000, **122:**5147-5157.
4. Braun M, Gmeiner J, Tzolov M, Coelle M, Meyer FD, Milius W, Hillebrecht H, Wendland O, Schutz JUV, Brutting W: **A new crystalline phase of the electroluminescent material tris(8-hydroxyquinoline) aluminum exhibiting blueshifted fluorescence.** *J Chem Phys* 2001, **114:**9625-9632.
5. Cölle M, Dinnebier RE, Brütting W: **The structure of the blue luminescent d-phase of tris(8-hydroxyquinoline)aluminium(III) (Alq_3).** *Chem Commun* 2002, **23:**2908-2909.
6. Cölle M, Gmeiner J, Milius W, Hillebrecht H, Brütting W: **Preparation and characterization of blue-luminescent tris(8-hydroxyquinoline)- aluminum (Alq_3).** *Adv Funct Mater* 2003, **13:**108-112.
7. Lin BC, Cheng CP, You ZQ, Hsu CP: **Charge transport properties of tris(8-hydroxyquinolinato)aluminum(III): Why it is an electron transporter.** *J Am Chem Soc* 2005, **127:**66-67.
8. Lesage A, Bardet M, Emsley L: **Through-bond carbon-carbon connectivities in disordered solids by NMR.** *J Am Chem Soc* 1999, **121:**10987-10993.
9. Kaji H, Schmidt-Rohr K: **Conformation and dynamics of atactic poly(acrylonitrile). 1. Trans/Gauche ratio from double-quantum solid-state ^{13}C NMR of the methylene groups.** *Macromolecules* 2000, **33:**5169-5180.
10. Utz M, Nandagopal M, Mathai M, Papadimitrakopoulos F: **Characterization of isomers in aluminium tris(quinoline-8-olate) by**

one-dimensional ^{27}Al NMR under magic angle spinning. *Appl Phys Lett* 2003, **83:**4023-4025.
11. Utz M, Nandagopal M, Mathai M, Papadimitrakopoulos F: **Chracterization of molecular diorder in vapor-diposited thin film of aluminium tris(quinoline-8-olate) by one-dimensional ^{27}Al NMR under magic angle spinning.** *J Chem Phys* 2006, **124:**0347051-0347058.
12. Bräuniger T, Poupko R, Luz Z, Gutsche P, Meinel C, Zimmermann H, Haeberlen U: **The dynamic disorder of azulene: A single crystal deuterium nuclear magnetic resonance study.** *J Chem Phys* 2000, **112:**10858-10870.
13. Bräuniger T, Poupko R, Luz Z, Zimmermann H, Haeberlen U: **Quantification of the orientational disorder in ortho-dichlorotetramethylbenzene: A single crystal deuterium nuclear magnetic resonance and x-ray study of the site populations.** *J Chem Phys* 2001, **115:**8049-8059.
14. Jerschow A: **From nuclear structure to the quadrupolar NMR interaction and high-resolution spectroscopy.** *Prog Nucl Magn Reson Spectrosc* 2005, **46:**63-78.
15. Medek A, Harwood JS, Frydman L: **Multiple-quantum magic-angle spinning NMR: A new method for the study of quadrupolar nuclei in solids.** *J Am Chem Soc* 1995, **117:**12779-12787.
16. Goldbourt A, Madhu PK: **Multiple-quantum magic-angle spinning: High-resolution solid state NMR spectroscopy of half-integer quadrupolar nuclei.** *Monatshefte für Chemie* 2002, **133:**1497-1534.
17. Goldbourt A, Madhu PK: **Multiple-quantum magic-angle spinning: High-resolution solid-state NMR of half-integer spin quadrupolar nuclei.** *Annu Rep NMR Spectrosc* 2004, **54:**81-153.
18. Laws DD, Bitter Hans-Marcus L, Jerschow A: **Solid-state NMR spectroscopic methods in chemistry.** *Angew Chem Int Ed* 2002, **41:**3096-3129.
19. Schurko RW, Wasylishen RE, Foerster H: **Characterization of anisotropic aluminum magnetic shielding tensors. Distorted octahedral complexes and linear molecules.** *J Phys Chem A* 1998, **102:**9750-9760.
20. Kaji H, Kusaka Y, Onoyama G, Horii F: **Relationships between light-emitting properties and different isomers in polymorphs of tris(8-hydroxyquinoline) aluminum(III) (Alq_3) analyzed by solid-state ^{27}Al NMR and Density Functional Theory (DFT) calculations.** *Jpn J Appl Phys* 2005, **44:**3706-3711.
21. Cramer CJ: *Essentials of Computational Chemistry-Theories and Models* Chichester: John Wiley and Sons; 2003.
22. Massiot D, Fayon F, Capron M, King I, Calve SL, Alonso B, Durand Jean-Olivier, Bujoli B, Gan Z, Hoatson G: **Modelling one- and two-dimensional solid-state NMR spectra.** *Magn Reson Chem* 2002, **40:**70-76.
23. Ravi Kishore VVN: **Photo-luminescence and electron-luminescence of hydroxy quinoline based organic semiconductors.** In *PhD Thesis* Tata Institute of Fundamental Research, Department of Chemical Sciences; 2004.
24. Vogel AI: *A Text Book of Quantitative Inorganic Analysis Including Elementary Instrumental Analysis* 3rd edition. New Delhi: ELBS; 1970.
25. Mucccini M, Loi MA, Kenevey K, Zamboni R, Masciocchi N, Sironi A: **Blue luminescence of facial tris(quinolin-8-olato)aluminum(III) in solution, crystals, and thin films.** *Adv Mater* 2004, **16:**861-864.
26. Brown SP, Wimperis S: **Two-dimensional multiple-quantum MAS NMR of quadrupolar nuclei. Acquisition of the whole echo.** *J Magn Reson* 1997, **124:**279-285.
27. Thakur RS, Kurur ND, Madhu PK: **Swept-frequency two-pulse phase modulation for heteronuclear dipolar decoupling in solid-state NMR.** *Chem Phys Lett* 2006, **426:**459-463.
28. Ganapathy S, Delevoye L, Amoureux J-P, Madhu PK: **Heteronuclear dipolar decoupling effects on multiple-quantum and satellite-transition magic-angle spinning NMR spectra.** *Magn Reson Chem* 2008, **46:**948-954.
29. Frisch MJ, Trucks GW, Schlegel HB, Scuseria GE, Robb MA, Cheeseman JR, Zakrzewski VG, Montgomery JA Jr, Vreven T, Kudin KN, Burant JC, Millam JM, Iyengar SS, Tomasi J, Barone V, Mennucci B, Cossi M, Scalmani G, Rega N, Petersson GA, Nakatsuji H, Hada M, Ehara M, Toyota K, Fukuda R, Hasegawa J, Ishida M, Nakajima T, Honda Y, Kitao O, Nakai H, Klene M, Li X, Knox JE, Hratchian HP, Cross JB, Bakken V, Adamo C, Jaramillo J, Gomperts R, Stratmann RE, Yazyev O, Austin AJ, Cammi R, Pomelli C, Ochterski JW, Ayala PY, Morokuma K, Voth GA, Salvador P, Dannenberg JJ, Zakrzewski VG, Dapprich S, Daniels AD, Strain MC, Farkas O, Malick DK, Rabuck AD, Raghavachari K, Foresman JB, Ortiz JV, Cui Q, Baboul AG, Clifford S, Cioslowski J, Stefanov BB, Liu G, Liashenko A, Piskorz P, Komaromi I, Martin RL, Fox DJ, Keith T, Al-Laham MA, Peng CY, Nanayakkara A, Challacombe M, Gill PMW, Johnson B, Chen W, Wong MW, Gonzalez C, Pople JA: Gaussian Inc., Wallingford CT; 2004.
30. Foresman JB, Keith TA, Wiberg KB, Snooria J, Frisch MJ: **Solvent effects. 5. Influence of cavity shape, truncation of electrostatics, and electron correlation on ab initio reaction field calculations.** *J Phys Chem* 1996, **100:**16098-16104.
31. Takahagi T, Saiki A, Sakaue H, Shingubara S: **Computer-aided chemistry estimation method of electronic-polarization dielectric constants for the molecular design of low-k materials.** *Jpn J Appl Phys* 2003, **42:**157-161.
32. Martin RL, Kress JD, Campbell IH, Smith DL: **Molecular and solid-state properties of tris-(8-hydroxyquinolate)-aluminum.** *Phys Rev B* 2002, **61:**15804-15811.
33. Schurko RW, Wi S, Frydman L: **Dynamic effects on the powder line shapes of half-integer quadrupolar nuclei: A solid-state NMR study of XO_4- Groups.** *J Phys Chem A* 2002, **106:**51-62.
34. Das D, Barbour LJ: **Polymorphism of a hexa-host: Isolation of four different single-crystal phases by melt crystallization.** *J Am Chem Soc* 2008, **130:**14032-14033.
35. Kello V, Sadlej AJ, Pyykko P, Sundholm D, Tokman M: **Electric quadrupole moment of the ^{27}Al nucleus: Converging results from the AlF and AlCl molecules and the Al atom.** *Chem Phys Lett* 1999, **304:**414-422.
36. Nishiyama Y, Fukushima T, Takami K, Kusaka Y, Yamazaki T, Kaji H: **Characterization of local structures in amorphous and crystalline tris(8-hydroxyquinoline) aluminum(III) (Alq_3) by solid-state ^{27}Al MQMAS NMR spectroscopy.** *Chem Phys Lett* 2009, **471:**80-84.